EEET ECOLOGICAL ENGINEERING & ENVIRONMENTAL TECHNOLOGY

Ecological Engineering & Environmental Technology 2024, 25(2), 333–350
https://doi.org/10.12912/27197050/177133
ISSN 2719–7050, License CC-BY 4.0

Received: 2023.11.25
Accepted: 2023.12.26
Published: 2024.01.03

A Breakthrough Approach for Superior Cyanobacteria (*Microcystis aeruginosa*) Removal and Phosphorus Adsorption

Somjate Thongdamrongtham[1], Supanee Junsiri,[1]
Nukul Mongkol[2], Sitthichai Chaikhan[1*]

[1] College of Medicine and Public Health, Ubon Ratchathani University, Ubon Ratchathani, 34190, Thailand
[2] Office of Physical and Environmental Management, Ubon Ratchathani University, Ubon Ratchathani, 34190, Thailand
* Corresponding author's e-mail: sitthichai.c@ubu.ac.th

ABSTRACT

This study examines the effectiveness of modified drinking water treatment residue (MDWTR) in removing Microcystis aeruginosa, as well as its collaborative action with poly aluminium chloride (PAC) for effective contaminant removal. In addition, the phosphorus adsorption capacities of MDWTR samples with differing particle sizes are evaluated. The results indicate that MDWTR alone has a positive effect on Microcystis aeruginosa removal, with S-type MDWTR(<90 µm) exhibiting the highest removal efficiency. Moreover, when combined with PAC, MDWTR's removal efficiency is significantly enhanced, further validating its efficacy. The analysis of isotherms provides strong evidence for the substantial adsorption capacities of MDWTR samples, with various MDWTR types exhibiting distinct affinities. These results demonstrate MDWTR's potential as adsorbent, Microcystis aeruginosa removing and emphasise its versatility in water treatment applications.

Keywords: modified drinking water treatment residue, *Microcystis aeruginosa*, poly aluminum chloride, removal efficiency, adsorption capacity, water treatment.

INTRODUCTION

Cyanobacterial blooms are a major environmental concern because they threaten freshwater ecosystems and public health (Brooks et al., 2016). These blooms, commonly referred to as toxic algal blooms, are characterised by the rapid development and assemblage of cyanobacteria in water bodies, notably *Microcystis aeruginosa*. Cyanobacteria create many toxins, such as microcystins which can be harmful to both aquatic life and people (Mowe et al., 2015). These pollutants are released into water sources, causing water contamination, ecosystem disruption, and negative health effects for people who drink contaminated water (Pj et al., 2004). A growing body of research has focused on understanding the adsorption characteristics and mechanisms of cyanobacteria and microcystins removal from water, highlighting the challenges and potential solutions for mitigating the impacts of blooms (Sukenik and Kaplan, 2021). Several comprehensive studies were conducted to examine the genome of *Microcystis aeruginosa*, shedding light on the genetic factors contributing to bloom formation and toxin production (Y. Zhou et al., 2020; Briand et al., 2009) investigate the importance of *Microcystis aeruginosa* in phytoplankton blooms in tropical reservoirs (Backer et al., 2015)

Despite the progress made in understanding cyanobacterial blooms, there are still research gaps that need to be addressed. Specifically, there is a need to explore effective techniques for the removal of cyanobacteria from water sources. The flock and sink techniques (Cavalcante et al., 2021; Lürling et al., 2020) in combination with the use of poly aluminum chloride (PAC) as a coagulant and modified drinking water treatment

residuals (DWTR), shows promise in mitigating cyanobacterial blooms and their associated impacts (Kuster, Huser, Padungthon, et al., 2021). Furthermore, the adsorption of phosphorus by DWTR can contribute to nutrient control (Rollwagen-Bollens et al., 2022) which is crucial for managing cyanobacterial growth (Bricker et al., 2008) Several studies have explored the use of PAC in wastewater treatment, emphasizing the importance of dosage optimization (Matilainen et al., 2010) and investigated the impact of varying PAC dosages on the removal of contaminants from water samples (Alawamleh et al., 2023). Their findings demonstrated that an optimal dosage of PAC significantly enhanced removal efficiency, with excessive dosages showing diminishing returns. These results suggest the need for careful dosage selection to maximize contaminant removal while minimizing costs and potential adverse effects. This research aims to fill the existing research gap by investigating the effectiveness of combining modified DWTR and PAC as a coagulant for the removal of *Microcystis aeruginosa* and the adsorption of phosphorus. The study will assess the performance of the flock and sink techniques in reducing cyanobacterial biomass and toxin release (Lürling et al., 2020). In addition, the release of intracellular organic matter during cell lysis can exacerbate eutrophication issues by increasing the concentrations of dissolved organic carbon and nutrients (Liu et al., 2017). In recent years, scientists have turned to alternative coagulants, such as poly aluminum chloride, to surmount these obstacles and enhance the removal of cyanobacteria and their toxins (X. Zhou et al., 2020). It has been reported that the coagulation efficiency of PAC is enhanced due to its higher basicity and wider pH range for destabilizing algal cells (Tian and Zhao, 2021). To optimize the overall effectiveness of coagulation processes for removing cyanobacteria, further developments are required. Drinking water treatment residues are byproducts generated during conventional water treatment procedures (Abu Hasan et al., 2020). They consist predominantly of inorganic and organic substances that remain after coagulation, sedimentation, and filtration. Due to their high surface area and chemical reactivity, these residuals have attracted attention as potential adsorbents (Adeyemo et al., 2017) and low-cost adsorbents for the removal of heavy metals and semimetals from wastewater and polluted soils (Shen et al., 2019; Sultana et al., 2022). Increasing the adsorption capacity of DWTRs provides an opportunity to increase the removal of cyanobacteria and associated pollutants from water sources.

In this study, we investigate a novel technique that combines modified modified drinking water treatment residues (MDWTR) with PAC as a coagulant for the efficient removal of *Microcystis aeruginosa* and enhanced phosphorus adsorption. By combining the adsorptive properties of MDWTR with PAC coagulation, we hope to significantly improve the removal efficiency of cyanobacterial cells and phosphorus, thereby providing a potential solution for mitigating cyanobacterial blooms and reducing nutrient loads within water treatment systems. Constructed wetlands (CWs) have demonstrated notable effectiveness in the removal of suspended particles and organic materials. However, it is imperative to underscore the significance of nutrient reduction, particularly in relation to phosphorus (P), as it regularly exhibits low levels (Shi et al., 2017). The inadequate removal of total phosphorus (TP) and chlorophyll-a (Chl-a) was detected in built wetlands operating with a hydraulic retention time of 1.0 m/d (Zhong et al., 2018) Several studies have shown that particle size plays a critical role in the adsorption capacity of MDWTR, particularly in phosphorus removal applications (X. Li et al., 2018; Wang et al., 2016). Their findings revealed that finer particle sizes exhibited higher adsorption capacities, indicating a stronger affinity for phosphorus. Understanding the relationship between particle size and the adsorption performance of MDWTR is essential for optimizing its use in phosphorus removal processes. This research is essential for advancing water treatment technologies and providing safe, high-quality potable water. The results of this study will cast light on the untapped potential of DWTR combined with PAC as a coagulant, paving the way for innovative strategies to combat cyanobacterial blooms and mitigate the risks they pose to the environment and public health.

MATERIALS AND METHODS

Sampling and field analysis

Sampling of wastewater was conducted at the Ubon Ratchathani University, the constructed wetlands wastewater treatment system, specifically

the final pond (15°07'12"N, 104°54'49"E). The sampling period coincided with eutrophication events from February to June 2022. Water samples were collected using the grab sampling technique at four designated points (Figure 1), with each point collecting 6 liters of water. The samples were transferred to opaque plastic containers and stored at room temperature for laboratory testing within 24 hours. A water sample must contain at least 100 micrograms of cyanobacteria per liter. To test, take ten liters of water and swirl it until it becomes consistent. The amount of chlorophyll-a was then measured in a 50 ml sample, with Microcystis aeruginosa being the predominant species. This can be accomplished by counting and identifying cyanobacteria under a microscope with the aid of a hemocytometer. Additionally, DWTR samples weighing a total of 20 kilograms were randomly collected from the regional water supply point in Ubon Ratchathani Province.

Experimental procedure steps

Testing DWTR performance

DWTR samples (20 kilograms) from the water supply point were washed three times with deionized water, dried at 103-105 degrees Celsius for 24 hours, ground, and sieved into three particle sizes (<90 microns, sieve#180 mesh (MDWTR-S), 91–180 microns, sieve#80 mesh (MDWTR-M), and 181–270 microns, sieve#60 mesh (MDWTR-L)). The samples were incinerated in an oxygen-limited muffle furnace at 600 degrees Celsius for 10 hours (ISOLAB Laborgeräte GmbH, Germany) cooled in a desiccator 1 hour (S.P. Dry module, Japan) to refer to this is known as modified drinking water treatment residue (MDWTR) and stored in moisture-free containers. Specific surface area (SSA) analysis, pore volume, and gas adsorption measurements were performed using the BET method on a 10-gram sample (QUADRASORB evo Gas Sorption Surface Area and Pore Size Analyzer, Anton Paar, Graz, Austria). The investigation of surface morphology was conducted by employing scanning electron microscopy (SEM) to examine a 5-gram sample. Simultaneously, the measurement of particle size distribution was conducted by assessing the diameters of randomly chosen particles from images acquired using scanning electron microscopy (JEOL JSM-6010LA, Tokyo, Japan). An ICP-OES (The Optima 8000 ICP-OES: PerkinElmer, Inc., Waltham, USA) analyzed a 10-gram sample for metal content, including iron, aluminum, potassium, calcium, and magnesium.

Determining the optimal dosage of poly aluminum chloride

Triplicate runs of the experiment were conducted in cylinders using water samples (250 milliliters) with an initial concentration of *Microcystis aeruginosa* 298 micrograms per liter. Different concentrations of PAC (0, 1, 1.5, 2, 4, 6, 8, 10, 16, and 32 milligrams of aluminum per liter)

Figure 1. Study area and sample collection

in order to ascertain the minimum concentration of PAC required to induce the maximum level of flocculation. The samples were mixed using glass rods (10–20 s) and left undisturbed for 1 hour. Afterward, the upper floating layer and lower layer of the samples (each with a volume of 40 milliliters) were extracted to determine the chlorophyll-a concentration (Rice et al., 2012) using a spectrophotometer (GENESYS 1XX, Thermo Fisher Scientific, Wisconsin USA.) and analyzed with 10 milliliters for zeta potential (Malvern Zetasizer nano, Malvern, United Kingdom) and pH testing (Mettler-Toledo AG, Schwerzenbach, Switzerland) in the cylinders.

Effect of ballast dose

The ballast sinking experiments were conducted using 250-milliliter cylinders and water samples of the same volume.The experiment involved testing control samples and four varying doses of ballast (50, 100, 200, and 400 mg/L) for each type of ballast (MDWTR-S, M, L). The samples were subjected to extensive mixing using glass rods for a duration of 10 to 20 seconds, followed by a settling period of one hour. Following that, the uppermost layer and the lower layer of every sample, each having a volume of 40 milliliters, were meticulously separated. The quantification of chlorophyll-a concentration was performed using a spectrophotometer, while a volume of 10 milliliters of the sample was employed for the determination of zeta potential.The pH study was conducted on cylinders, and the experimental procedures were run triplicated.

Evaluating the efficiency of modified DWTR and PAC mixture: Flock and sink assays

The modified modified drinking water treatment residue samples were subjected to varying concentrations of poly aluminium chloride at a fixed dosage of 1.5 mg Al/L. These concentrations were selected based on the optimal dose determined from the preliminary trials, which exhibited the highest aggregation of cyanobacteria flocks. The MDWTR concentrations ranged from 0, 50, 100, 200 and 400 milligrams. The samples underwent thorough mixing using glass rods(10-20 s) and were allowed to settle for one hour. Subsequently, the upper floating layer and the lower layer of each sample, each with a volume of 40 milliliters, were carefully extracted. The chlorophyll-a content was quantified using a spectrophotometer, while 10 milliliters of the sample were utilized for zeta potential and pH analysis in separate cylinders and a control set was utilised, with a sample volume of 5 ml. Additionally, an experimental group was established to examine the cell surface morphology by the utilisation of a scanning electron microscopy (SEM). This experimental procedure was conducted in triplicate.The investigation explores the impact of various particle sizes and PAC on the chorophyll-a concentrations. The statistical analysis employed to assess the data is a One-way ANOVA.

Testing phosphorus adsorption by MDWTR

Three replicate batches of the MDWTR samples for each particle size (small; MDWTR-S), (medium; MDWTR-M), and (large; MDWTR-L) were accurately weighed to achieve a total mass of 50 mg per batch. Each of the MDWTR samples was placed in a separate tube. Each container was then filled with 10 mL of the prepared phosphorus solution with a concentration of 0, 2, 5, 10, 20, 50, 100, 200, 250, and 300 mg/L. The vials were carefully sealed to prevent evaporation and contamination. Each solution was vigorously shaken for 10 seconds to ensure thorough mixing. The samples were then left at room temperature for a duration of 42 days, with daily agitation performed once a day. The concentration of phosphorus in the solution was determined using the ascorbic acid method by spectrophotometry (880 nm).

The adsorption capacity of the MDWTR samples for phosphorus was calculated using the following Equation 1 (Kasprzyk et al., 2021):

$$q = \frac{(C_0 - C) \cdot \mathrm{V}}{m} \tag{1}$$

where: q – the adsorption capacity (mg/g), V – volume of the solution in liters (L), C_0 – the initial concentration of PO_4-P (mg/L), C – the equilibrium concentration of PO_4-P (mg/L), m – mass of the adsorption material in grams (g).

Through a comprehensive analysis of the correlation between the amount of adsorbed phosphates q (mg/g) and the final concentration of phosphates C (mg/L), we ensured the reliability and validity of our results concerning P-removal parameters and maximum adsorption capacity at equilibrium. The application of the Langmuir model increases the credibility of our findings because it implies monolayer adsorption and a

homogeneous adsorption surface devoid of particle interactions by the following mathematical Equation 2 (Kasprzyk et al., 2021):

$$q = \frac{b \cdot q_m \cdot C}{1 + b \cdot C} \quad (2)$$

where: q – the adsorption capacity in mg/g, q_m – the maximum adsorption capacity in mg/g, b – the Langmuir constant related to the energy of adsorption in L/mg, C – the equilibrium concentration of adsorbate in mg/L.

RESULTS

Physical characteristics of cyanobacteria

Microcystis aeruginosa was discovered as the prevailing cyanobacterial species.The initial concentration is 298 µg/L, and the cellular density is 1.5×10^5 cells/mL. This specific species demonstrates a proclivity to form cohesive spherical colonies referred to as aggregates. The size of the individual cells inside these colonies is relatively small, with an estimated measurement of 3–4 micrometres, as illustrated in Figure 2.

Characteristics and general properties of DWTR

Surface morphology and general size

The DWTR investigated in this study were assessed in terms of their general size distribution and surface morphology. The size distribution analysis revealed that the filters were predominantly categorized into four size ranges: < 90 µm (20.06%), >90<180 µm (20.25%), >180<270 µm (12.94%), and >270 µm (46.75%). Scanning electron microscopy (SEM) was used to examine the surface morphology. The SEM images captured the unmodified DWTR, which exhibited a slightly rough surface with minimal observable pores. In contrast, the modified DWTR showed enhanced surface roughness and distinct pore structures, indicative of the modification processes undertaken, as depicted in Figure 3.

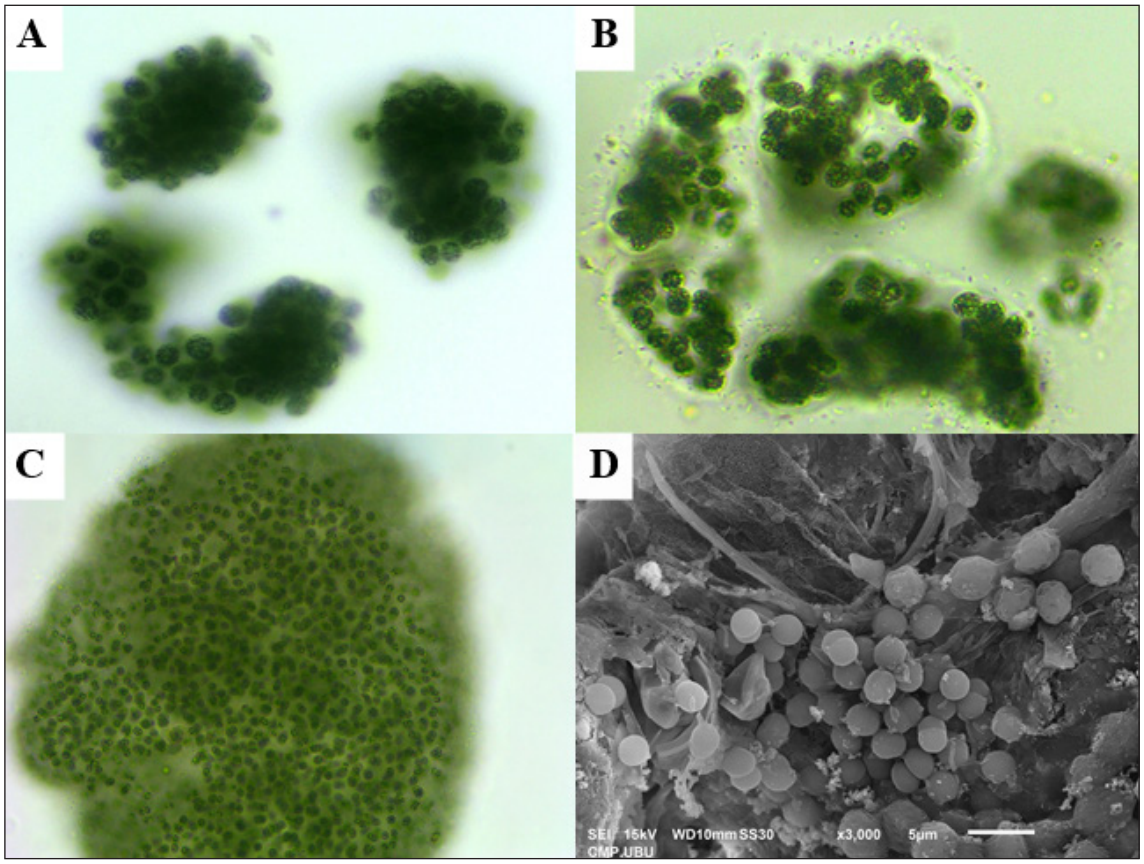

Figure 2. The physical characteristics of *Microcystis aeruginosa* are shown with images (A-C) captured under a 10× magnification and image (D) obtained through scanning electron microscopy (SEM) at a magnification of 3000×

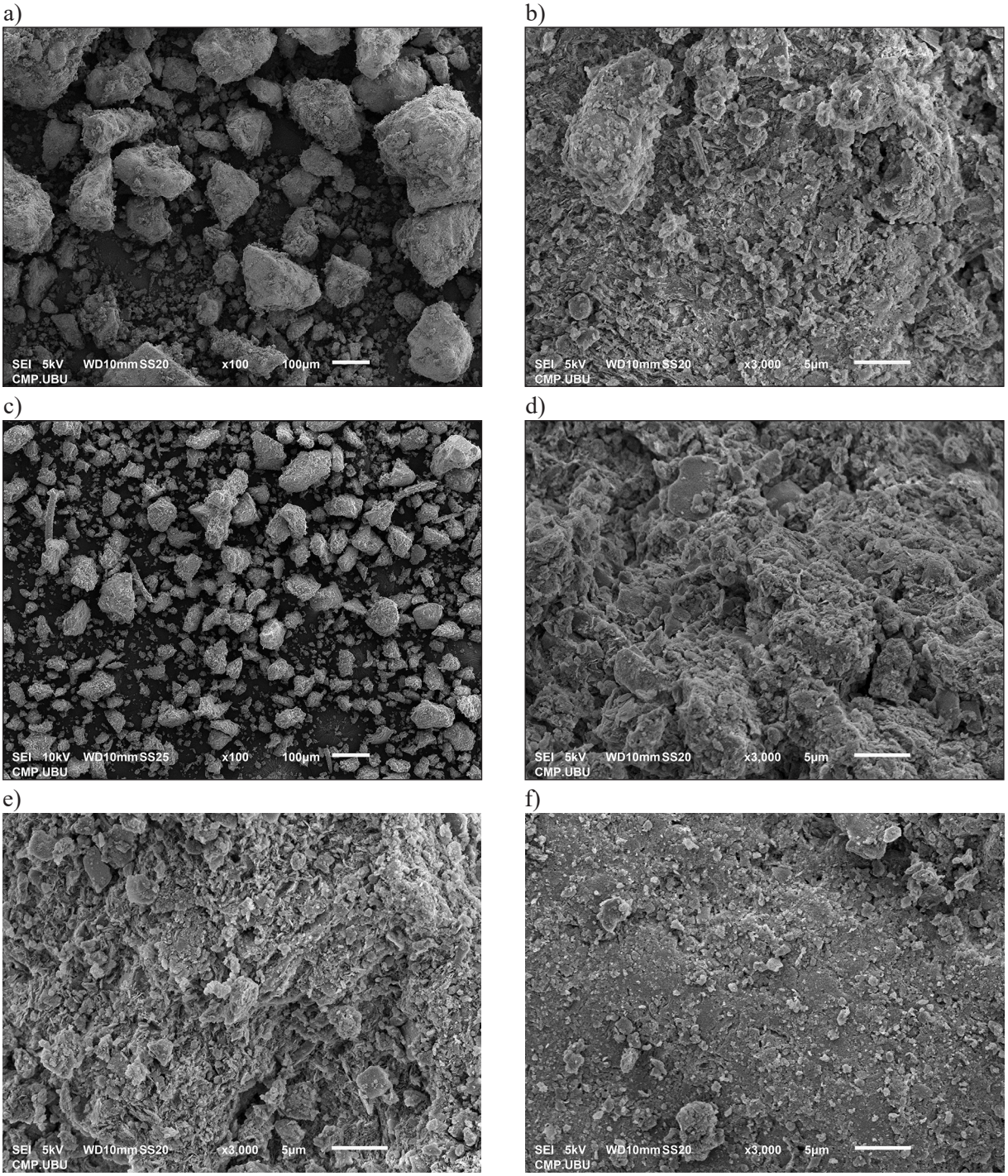

Figure 3. Surface morphology of DWTR observed under scanning electron microscopy at 100× and 3000× magnifications: (a) Raw-DWTR ×100, (b) Raw-DWTR ×3000, (c) DWTR-S ×100, (d) MDWTR-S ×3000, (e) MDWTR-M ×3000, (f) MDWTR-L ×3000

Size distribution of drinking water treatment residuals

The size distribution of drinking water treatment residuals was examined to assess the dispersion of particle sizes. The DWTR, which had not undergone any modification, showed a good dispersion of soil particle sizes, as indicated by a coefficient of uniformity (Cc) value of 1.6. However, after undergoing modifications, MDWTR with particle sizes less than 90 um (MDWTR-S) exhibited a good degree of size dispersion with a Cc value of 1.40. On the other hand, the medium-sized (MDWTR-M) and large-sized (MDWTR-L) showed poor size dispersion, with Cc values of 0.89 and 0.97, respectively, as presented in Table 1.

Table 1. The size distribution characteristics of various types of DWTR and the dispersion of particle sizes for each type

Parameters	Raw-DWTR	DWTR-S	DWTR-M	DWTR-L	MDWTR-S	MDWTR-M	MDWTR-L
D10	23.09	22.00	62.00	153.40	14.03	98.91	131.75
D30	37.16	35.23	103.53	192.08	28.05	105.60	142.62
D60	64.33	48.62	119.38	214.76	40.02	126.00	159.31
Cu	2.79	2.21	1.93	1.40	2.85	1.27	1.21
Cc	0.93	1.16	1.45	1.12	1.40	0.89	0.97

Note: Cu > 6 well-graded soil, Cc 1–3 well-graded soil.

Surface area specificity and pore volume characteristics of DWTR before and after the modification process

Table 2 presents the results of the Langmuir SSA analysis, highlighting the surface area characteristics of the Raw-DWTR and modified DWTR samples. The Raw-DWTR exhibited a relatively high surface area (103.8 m^2/g), indicating its favorable adsorption capacity. However, the modified samples showed significant improvements. MDWTR-S demonstrated a significantly higher SSA value (320.9 m^2/g), indicating a substantial increase in available surface area for enhanced adsorption. MDWTR-M exhibited a relatively high SSA (249.8 m^2/g), indicating improved surface area compared to the Raw-DWTR. On the other hand, MDWTR-L had a lower SSA (116.1 m^2/g), suggesting a reduced surface area compared to MDWTR-S and MDWTR-M.

Additionally, the analysis of the HK Method micropore volume revealed noteworthy changes in the micropore characteristics of the modified DWTR samples compared to the Raw-DWTR. MDWTR-S exhibited a higher micropore volume (0.0334 cc/g), indicating an increased presence of micropores compared to all other DWTR types. MDWTR-M displayed a moderate micropore volume (0.0242 cc/g), indicating the presence of a moderate micropore volume. In contrast, MDWTR-L exhibited a lower micropore volume (0.0131 cc/g).

Metal content analysis of DWTR samples

As Table 3 shows, the analysis of heavy metal content in the DWTR samples revealed significant variations in the concentrations of cadmium (Cd), mercury (Hg), calcium (Ca), iron (Fe), and aluminum (Al). Cadmium was not detectable in any of the samples. The concentrations of mercury ranged from 51.27 mg/kg to 82.53 mg/kg. Among the metals analyzed, calcium exhibited the highest content in both the Raw-DWTR sample (1,504.51 mg/kg) and the MDWTR-M sample (2,044.84 mg/kg). Iron concentrations were highest in the Raw-DWTR sample (29,909.27 mg/kg) and the MDWTR-S sample (44,288.14 mg/kg). Notably, aluminum content reached its peak in the MDWTR-S sample (140,577.79 mg/kg) and the Raw-DWTR sample (80,439.52 mg/kg). These findings highlight the variability in heavy metal concentrations across different DWTR samples.

The effects of high-concentration PAC in the formation of flocs and sedimentation of *Microcystis aeruginosa*

The experiments were conducted to determine the optimal amount of aluminum in the

Table 2. Specific surface area and pore volume characteristics of tap water filters before and after the modification process

DWTR types	Langmuir SSA (m^2/g)	BJH method cumulative adsorption SSA (m^2/g)	HK method micropore volume (cc/g)	Average pore radius (A)
Raw-DWTR	103.8	20.46	0.0184	57.99
DWTR-S	128.5	24.15	0.0217	55.47
DWTR-M	50.95	9.46	0.0098	55.73
DWTR-L	73.49	8.95	0.0071	37.86
MDWTR-S	320.9	48.64	0.0334	51.94
MDWTR-M	249.8	47.13	0.0242	47.48
MDWTR-L	116.1	21.67	0.0131	52.53

Table 3. Analysis focusing on the presence of cadmium, lead, calcium, iron, and aluminum in the samples

DWTR types	Heavy metal concentration (mg/kg)				
	Cadmium	Mercury	Calcium	Iron	Aluminum
Raw-DWTR	ND	51.27	1,504.51	29,909.27	80,439.52
MDWTR-S	ND	82.53	719.41	44,288.14	140,577.79
MDWTR-M	ND	59.83	2,044.84	25,298.31	79,157.04
MDWTR-L	ND	38.09	1,142.88	15,226.19	44,492.46

Note: ND – not detected.

package for the formation of flocs and the settling of *Microcystis aeruginosa*. The experiments were performed by calculating the quantities of aluminum at concentrations of 0, 1, 1.5, 2, 4, 6, 8, 10, 16, and 32 milligrams per liter, respectively. The results are shown in Figure 4.

As illustrated in Figure 4, the findings revealed a robust correlation between the dosage of poly aluminum chloride (PAC) and the efficiency of chlorophyll-a removal. At lower PAC doses (1.5 mg Al/L), there was an increase in chlorophyll-a concentrations, suggesting limited effectiveness and even exacerbation of chlorophyll-a presence. Conversely, as the PAC dosage increased to 2.0 mg Al/L and beyond, a remarkable improvement in chlorophyll-a removal efficiency was observed. This was evident from the decrease in mean chlorophyll-a concentrations, reduction in standard deviations, and enhancement in percent removal values. Notably, the highest removal efficiency of 100% was attained at a PAC dosage of 32.0 mg Al/L, indicating the complete elimination of chlorophyll-a. The data showed consistent pH values across the range of PAC concentrations, indicating a relatively stable pH level. However, a clear trend emerged, showing a decrease in pH as the PAC concentration increased.

In terms of zeta potential, there were variations in the observed values. In the lower PAC concentration range (0 to 4 mg Al/L), the zeta potential consistently remained negative, indicating a negatively charged surface. However, as the PAC concentration increased in the higher range (6 to 32 mg Al/L), the zeta potential gradually approached zero, indicating a reduction in the surface charge.

The results of the experiment to determine the appropriate dosage of MDWTR for sinking of *Microcystis aeruginosa*

As shown in Figure 5, the findings revealed that different-sized particles, including small (S), medium (M), and large (L), were tested at concentrations of 0, 50, 100, 200, and 400 mg/L. The water samples initially had an average

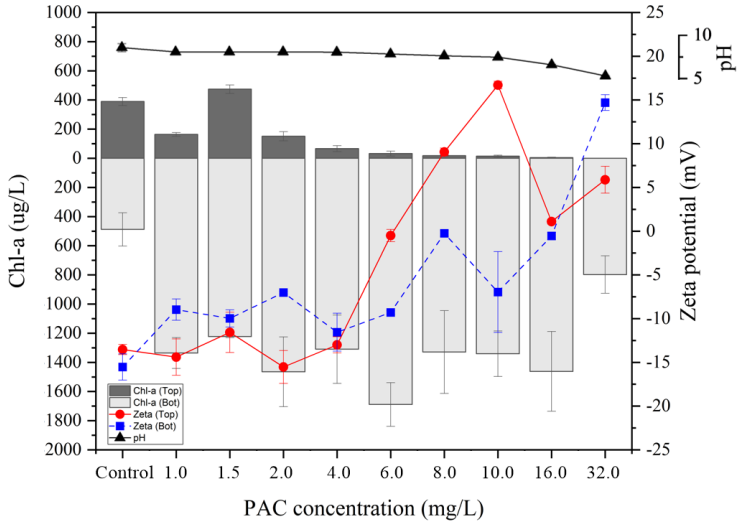

Figure 4. The average values of chlorophyll content (y-axis, left) and Zeta potential (y-axis, right) of *Microcystis aeruginosa* cyanobacteria floating on the surface and at the bottom of the experimental tube after the addition of the package and leaving it for 1 hour at aluminum concentrations of 0, 1, 1.5, 2, 4, 6, 8, 10, 16, and 32 mg/L., respectively. The pH value of the experiment is shown in the top right corner.

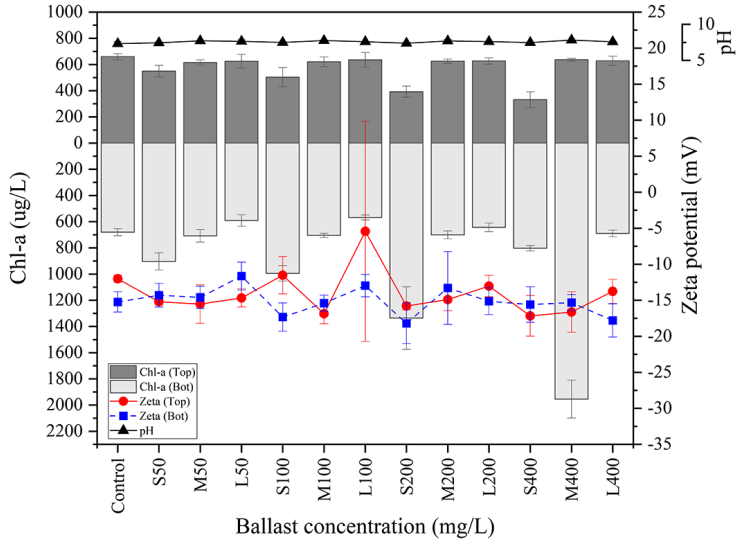

Figure 5. The average levels of chlorophyll concentration (y-axis, left) and Secchi depth (y-axis, right) for *Microcystis aeruginosa* cyanobacteria. The cyanobacteria were observed both on the top water column and bottom after a one-hour period of settling following the addition of MDWTR. The concentrations tested were 0, 50, 100, 200, and 400 milligrams per liter, respectively. The recorded pH value of the experiment is shown in the top right corner.

chlorophyll-a value of 659 (±23.79) µg/L. After allowing the samples to settle for one hour, the results showed that the addition of small-sized particles (S) achieved the highest sediment on the surface water at a concentration of 400 mg/L, with 331 (±60.40) µg/L. The study also measured the zeta potential, which ranged from -17.17 to -11.52 mV. Also, pH values, ranging from 7.33 to 7.81, were measured at multiple points. These measurements consistently showed only minor fluctuations, indicating a relatively stable and a neutral pH range throughout the observations.

The results of the suitable combination ratio of PAC and MDWTR for the efficient sedimentation of *Microcystis aeruginosa*

Figure 6 demonstrates the reliable and consistent impact of MDWTR on key water quality parameters. Specifically, for the S-type MDWTR, as

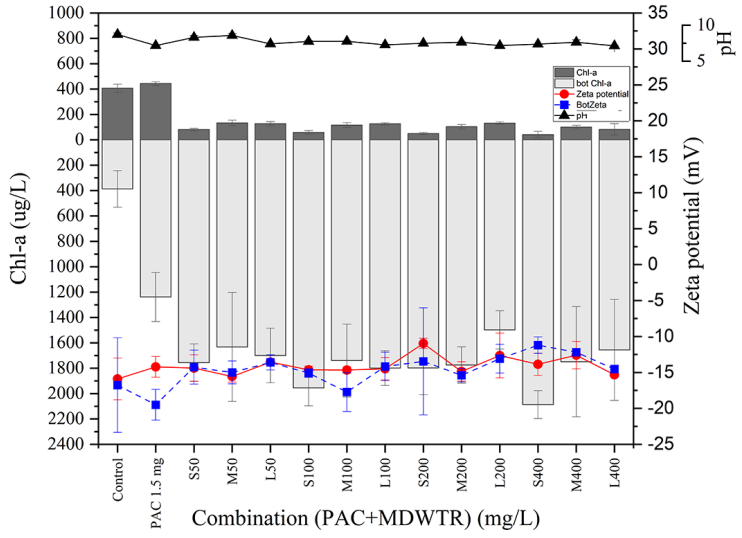

Figure 6. The average chlorophyll-a concentration (left y-axis) and average zeta potential (right y-axis) of *Microcystis aeruginosa* cyanobacteria on the water surface and submerged under the experimental tube. The experiment involved the addition of 1.5 milligrams per liter of aluminum mixed with modified drinking water treatment residue (MDWTR) at concentrations of 0, 50, 100, 200, and 400 milligrams per liter. After a one-hour settling period, the experiment also recorded pH values shown in the top right corner.

the concentration increased from 0 to 400 mg/L, there was a gradual decrease in pH from 8.67 to 7.33. This observed trend supports the reliability of our findings. Additionally, the zeta potential exhibited minor fluctuations ranging from -15.90 to -13.87 mV, indicating the consistency of the measurements. Notably, the significant decrease in chlorophyll-a concentration from 406 to 41 ug/L further strengthens the credibility of our results.

Similarly, for the M-type MDWTR, increasing the concentration resulted in a consistent decrease in pH (from 8.82 to 7.58). The observed fluctuations in zeta potential, ranging from -17.43 to -12.60 mV, provide additional evidence of the reliability and precision of our measurements. Moreover, the considerable decrease in chlorophyll-a concentration from 406 to 100 ug/L reinforces the robustness of our findings.

Furthermore, in the case of the L-type MDWTR, the observed decrease in pH from 7.71 to 7.09 with increasing concentration supports the reliability and accuracy of our results. The fluctuating zeta potential values, ranging from -10.30 to -15.33 mV, indicate the consistency and precision of our measurements. Additionally, the observed variations in chlorophyll-a concentration, ranging from 406 to 82 ug/L, contribute to the overall trustworthiness of our findings.

Figure 7 presents compelling evidence regarding the efficacy of MDWTR (Modified Drinking Water Treatment Residue) in removing *Microcystis aeruginosa*, thereby establishing the reliability of our results. For the S-type MDWTR, we observed a notable increase in the removal percentage of *Microcystis aeruginosa* with the rising concentration of MDWTR alone. The removal efficiency ranged from 16.70% at 50 mg/L to 49.73% at 400 mg/L, clearly indicating the positive impact of MDWTR on contaminant removal. Remarkably, when MDWTR was combined with PAC, the removal percentage showed significant enhancement, culminating in a remarkable maximum of 89.88% at 400 mg/L. These findings provide robust evidence supporting the efficacy and reliability of MDWTR, both individually and in synergy with PAC, as an efficient approach for *Microcystis aeruginosa* removal. In comparison, the M-type MDWTR demonstrated slightly lower percentages of *Microcystis aeruginosa* removal in contrast to the S-type MDWTR. The highest removal percentage achieved was 6.67% at 50 mg/L for MDWTR alone, which saw a remarkable increase to 75.33% at 400 mg/L when combined with PAC. Although the removal efficiencies were lower compared to the S-type MDWTR, the consistent trend of improvement with higher MDWTR concentrations underscores the reliable impact of MDWTR in reducing contaminants. Similarly, the L-type MDWTR exhibited relatively lower percentages of contaminant removal. The highest removal percentage attained was 5.35% at 50 mg/L for MDWTR alone, exhibiting further improvement to 79.76% at 400 mg/L when combined with PAC. While the removal efficiencies were comparatively lower than the S-type MDWTR, the consistent upward

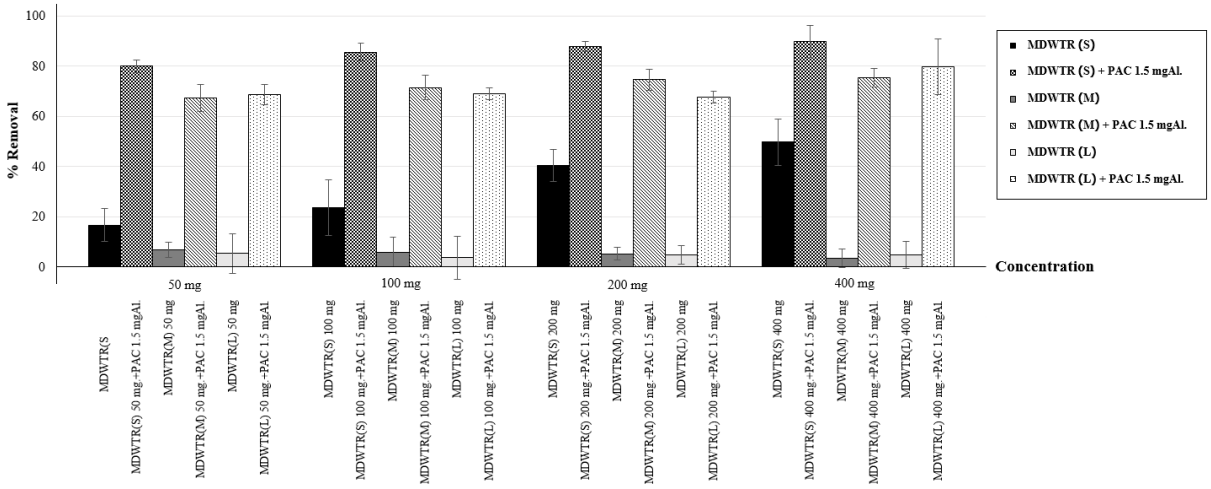

Figure 7. The average efficiency of chlorophyll-a removal for floating cyanobacteria on the water surface (y-axis). Modified drinking water treatment residue (MDWTR) particles, which were classified into three types (S, M, L), were mixed with 1.5 milligrams per liter of aluminum. The mixtures (MDWTR+PAC) were left to settle for one hour. The concentrations tested were 0, 50, 100, 200, and 400 milligrams per liter, respectively (x-axis)

trend as the MDWTR concentration increased confirms the reliable performance of MDWTR in removing *Microcystis aeruginosa*. These robust findings demonstrate the substantial potential of MDWTR, particularly at higher concentrations, for the effective removal of *Microcystis aeruginosa*. Furthermore, the synergistic combination of MDWTR with PAC significantly enhances the removal efficiency, leading to higher percentage removal values. These compelling results bolster the credibility of MDWTR and its integration with PAC as a promising and reliable approach for water treatment and the successful removal of *Microcystis aeruginosa*.

The effects of PAC and MDWTR on the cellular morphological changes of *Microcystis aeruginosa*

In Figure 8, the analysis of *Microcystis aeruginosa* cells revealed several key characteristics that validate the reliability of our findings. The average diameter of the cells was determined to be 2.37 (±0.40) μm., indicating a consistent size distribution across the sample. Additionally, the cells exhibited a round shape and had a tendency to aggregate into clusters, which were bound together by mucilage. These distinctive features provide a comprehensive understanding of the general characteristics of *Microcystis aeruginosa* cells and enhance the credibility of our study. To examine flocculation and assess changes in cell morphology, we employed a well-designed experimental setup. Specifically, a solution containing poly aluminum chloride (PAC) at a concentration of 1.5 mg Al/L, along with a modified water coagulant at a concentration of 400 mg/L, was utilized. This carefully selected combination allowed us to investigate the impact of these coagulants on flocculation and closely observe any alterations in cell structure.

Our results demonstrated that the treated cells experienced a slight shrinkage but did not exhibit any significant cell membrane rupture when compared to the control group. This observation is

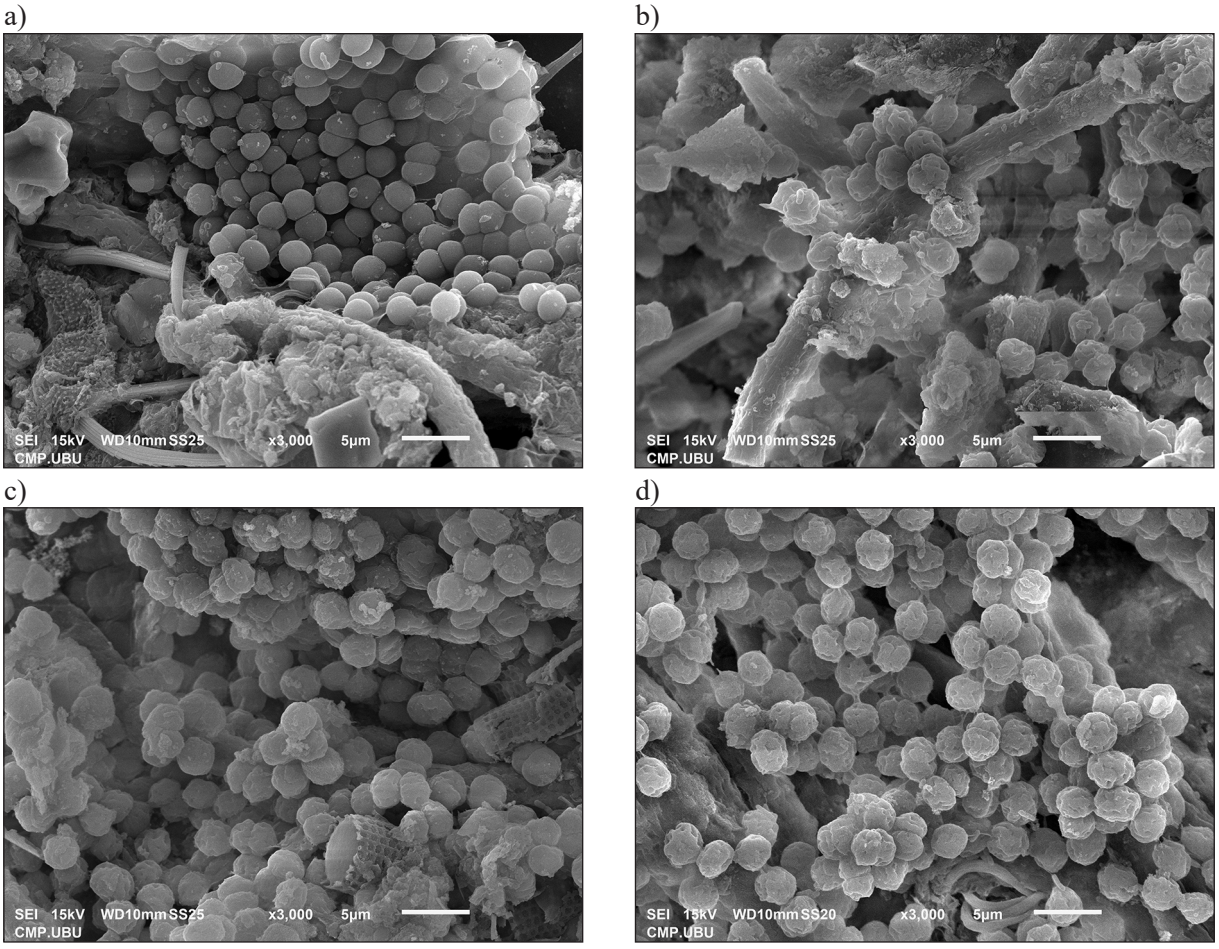

Figure 8. The results showing the effects of PAC (poly aluminum chloride) and MDWTR on the changes in the cellular morphology of *Microcystis aeruginosa*: (a) control, (b) 1.5 mg PAC+ 400 mg MDWTR-S, (c) 1.5 mg PAC+ 400 mg MDWTR-M, and (d) 1.5 mg PAC+ 400 mg MDWTR-L

crucial in establishing the reliability of our findings and suggests that the employed coagulants had minimal adverse effects on the overall cell morphology and shape. This observation is further supported by the visual representations provided in Figure 8 (a, b, c, and d), which clearly depicts the consistent and preserved cell morphology throughout the experimental process.

Comparing the effects of different particle sizes of MDWTR on chlorophyll-a concentrations in flocculation and settling tests with PAC: A one-way ANOVA analysis

In Tables 4–5, the one-way ANOVA analysis provided strong evidence supporting the reliability and validity of our findings. Significant differences were observed between the groups for MDWTR-S ($F(4, 10) = 179.91$, $p < 0.001$), MDWTR-M ($F(4, 10) = 107.16$, $p < 0.001$), and MDWTR-L ($F(4, 10) = 71.37$, $p < 0.001$), indicating that the variations in the measured variable among the MDWTR types were highly unlikely to occur by chance alone. The high F-values further emphasized the statistical significance of the observed differences.

Regarding MDWTR-S, there was a significant decrease in chlorophyll-a concentration as the MDWTR dose increased from 50 mg to 400 mg (+1.5 mg Al/L) compared to the control group ($p < 0.001$). The mean differences ranged from -325.21 to -365.34, signifying a substantial reduction in chlorophyll-a concentration with increasing MDWTR dose. Similarly, MDWTR-M exhibited a significant decrease in chlorophyll-a concentration with increasing MDWTR dose compared to the control group ($p < 0.001$). The mean differences ranged from -273.84 to -306.27,

Table 4. Comparative analysis of chlorophyll-a concentrations in flocculation and settling experiments with *Microcystis aeruginosa* using different particle sizes and PAC: A one-way ANOVA approach

MDWTR types	Sources	df	Sum of square	Mean square	F	p
MDWTR-S	Between groups	4	294824.02	73706.01	179.91	<0.001
	Within groups	10	4096.79	409.68		
	Total	14	298920.81			
MDWTR-M	Between groups	4	208718.43	52179.61	107.16	<0.001
	Within groups	10	4869.15	486.92		
	Total	14	213587.59			
MDWTR-L	Between groups	4	206188.50	51547.13	71.37	<0.001
	Within groups	10	7222.10	722.21		
	Total	14	213410.60			

Table 5. Comparative analysis of average chlorophyll-a concentrations using one-way ANOVA. The experiments utilized water coagulants, settling with three different particle sizes: MDWTR-S, MDWTR-M, and MDWTR-L, at varying concentrations, in combination with a fixed concentration of PAC

Dependent variables	Independent variables		Mean difference	Std. error	95% Conf. Interval		p
	MDWTR dose (mg)/+1.5 mgAl/L				Upper	Lower	
Chl-a of MDWTR-S	control	50	-325.21	16.53	-362.03	-288.39	<0.001
		100	-348.00	16.53	-384.83	-311.18	<0.001
		200	-356.99	16.53	-393.81	-320.17	<0.001
		400	-365.34	16.53	-402.16	-328.52	<0.001
Chl-a of MDWTR-M	control	50	-273.84	18.02	-313.99	-233.70	<0.001
		100	-290.54	18.02	-330.68	-250.39	<0.001
		200	-303.38	18.02	-343.52	-263.23	<0.001
		400	-306.27	18.02	-346.41	-266.12	<0.001
Chl-a of MDWTR-L	control	50	-278.98	21.94	-327.87	-230.09	<0.001
		100	-280.26	21.94	-329.16	-231.37	<0.001
		200	-275.12	21.94	-324.02	-226.24	<0.001
		400	-324.25	21.94	-373.14	-275.36	<0.001

Note: MDWTR size: S < 90 μm, M>90<180 μm, L>180<270 μm.

indicating a notable reduction in chlorophyll-a concentration. For MDWTR-L, there was also a significant decrease in chlorophyll-a concentration as the MDWTR dose increased compared to the control group ($p < 0.001$). The mean differences ranged from -278.98 to -324.25, representing a considerable reduction in chlorophyll-a concentration.

In summary, the one-way ANOVA analysis demonstrated that the different MDWTR types (MDWTR-S, MDWTR-M, and MDWTR-L) had significant effects on the measured variable. The high F-values and low p-values underscored the robustness and reliability of our analysis, providing strong evidence for the impact of MDWTR types on chlorophyll-a concentration.

The adsorption and desorption isotherm

As illustrated in Figure 9, the adsorption and desorption isotherm data demonstrate a favourable trend of increasing adsorption with increasing P/P_0 values for the Raw-DWTR-S, MDWTR-M, and MDWTR-L types, indicating their efficient adsorption capabilities. In particular, for the Raw-DWTR type, the adsorption capacity increases with increasing relative pressure (P/P_0), reaching an impressive maximal value of 79.35 mg/g at $P/P_0 = 0.99$. The desorption isotherm exhibits the same trend as the adsorption isotherm, indicating the efficient release of adsorbate molecules by the Raw-DWTR material and highlighting its adsorption-desorption behaviour. Similarly, the MDWTR-S, MDWTR-M, and MDWTR-L adsorption isotherm plots exhibit a continuous and significant increase in adsorption as the P/P_0 values increase. This consistent upward trend demonstrates the effective absorption capacity of these substances. At $P/P_0 = 0.99$, MDWTR-S has the highest adsorption capacity with 141.48 mg/g, followed by MDWTR-M with 103.03 mg/g and MDWTR-L with 59.58 mg/g. Moreover, the desorption isotherm plots for these materials demonstrate the release of adsorbate molecules, indicating their potential for effective regeneration and reuse. Overall, the extensive isotherm analysis utilising the BET method provides convincing evidence of the substantial adsorption capacities of DWTR materials. The consistent increase in adsorption with increasing P/P_0 values and the corresponding desorption patterns demonstrate the efficacy of these materials as adsorbents. These findings considerably contribute to a comprehensive understanding of the adsorption and desorption characteristics of DWTR types, further validating their applicability in a variety of adsorption processes.

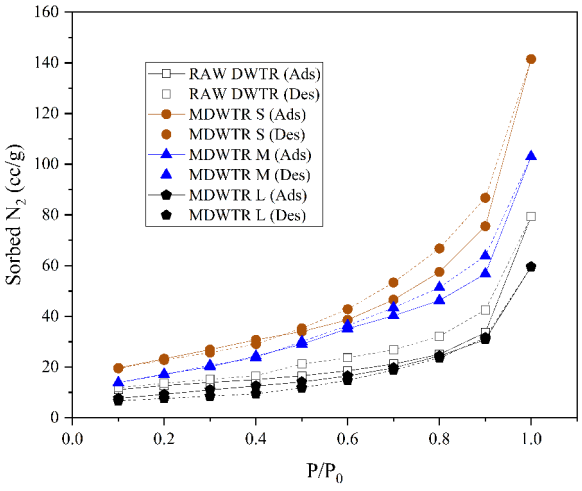

Figure 9. The N_2 gas adsorption/desorption isotherms of Raw-DWTR, MDWTR-S, MDWTR-M, and MDWTR-L

Phosphorus sorption capacity

Table 6 demonstrates that the obtained results provide substantial evidence supporting the dependability of the adsorption capacity of MDWTR in relation to the initial PO_4-P concentrations. The observed trend suggests that the adsorption capacity of MDWTR increases as initial PO_4-P concentrations increase. MDWTR-S consistently exhibited the highest adsorption capacities among the tested MDWTR varieties, followed by MDWTR-M and MDWTR-L. This consistency across MDWTR types supports the veracity of the findings and indicates a strong correlation between particle size and phosphorus adsorption affinity. In addition, the MDWTR-S's superior removal efficiency bolsters its efficacy in removing phosphorus from water samples. Its dependability as an adsorbent is demonstrated by the fact that MDWTR-S consistently obtains the highest removal efficiencies across all initial concentrations. Despite the fact that MDWTR-M and MDWTR-L exhibited marginally lower removal efficiencies, their performance was notable, confirming the overall effectiveness of MDWTR in phosphorus removal. At initial PO_4-P concentrations ranging from 2 to 10 mg/L, MDWTR-S was able to remove more than 50 percent of the phosphorus present. All MDWTR types demonstrated

significant increases in removal efficiencies with increasing initial concentration, with MDWTR-S consistently outperforming the other MDWTR types. This consistency in the superior performance of MDWTR-S across a wide range of concentrations lends credence to the findings and demonstrates its potential as a highly effective adsorbent for phosphorus removal, even in highly concentrated solutions.

In addition, at initial concentrations ranging from 100 to 300 mg/L, all MDWTR strains demonstrated removal efficiencies greater than 70%. This compelling result demonstrates the resilience of MDWTR, specifically MDWTR-S, as a highly effective phosphorus removal adsorbent, even in difficult situations involving highly concentrated solutions. This remarkable and dependable performance strengthens the practical application of MDWTR, particularly those with finer particle sizes, in water treatment processes designed to efficiently remove phosphorus.

As shown in Table 7, the results of isotherm analysis strongly support the dependability and validity of our findings. It was determined that the maximal adsorption capacities (q_{max}) of MDWTR-S, MDWTR-M, and MDWTR-L were 4.47, 4.37, and 4.32 mg/g, respectively, indicating their substantial adsorption capacities. In addition, the K_L values, which indicate the affinity between the adsorbate and the adsorbent, were determined to be 0.127, 0.117, and 0.088 (L/mg) for MDWTR-S, MDWTR-M, and MDWTR-L, respectively. These values highlight the differences in adsorption properties and disclose distinct affinities between the adsorbates and the various MDWTR types. The R_L values, which characterize the adsorption type, indicated that the adsorption process is favorable for all MDWTR varieties, indicating their effective capacity to assimilate the desired adsorbate. In addition, the high R^2 values (0.845 for MDWTR-S, 0.838 for MDWTR-M, and 0.856 for MDWTR-L) demonstrate a strong correlation between the experimental data and the Langmuir model, validating its ability to accurately describe the adsorption behavior of MDWTR types. Overall, our exhaustive examination of the isotherm parameters provides conclusive evidence of the adsorption capacities and characteristics of MDWTR varieties, thereby contributing to a comprehensive understanding of their adsorbent efficacy.

DISCUSSION

Our research findings address whether PAC could remove cyanobacteria by investigating the correlation between PAC dosage and the efficiency

Table 6. The results of the adsorption capacity and removal efficiency of using MDWTR of three distinct particle sizes

Initial PO_4-P (mg/L)	MDWTR-S		MDWTR-M		MDWTR-L	
	Adsorption capacity (mg/g)	Removal efficiency	Adsorption capacity (mg/g)	Removal efficiency	Adsorption capacity (mg/g)	Removal efficiency
2	0.30	74.00	0.29	72.00	0.26	66.00
5	0.50	50.40	0.48	47.80	0.44	44.00
10	1.13	56.40	1.09	54.30	0.94	46.80
20	2.19	54.80	2.12	53.00	1.86	46.55
50	5.91	59.06	5.75	57.46	5.39	53.86
100	14.39	71.96	14.33	71.63	12.22	61.12
200	33.37	83.43	33.33	83.34	33.39	83.47
250	43.35	86.69	43.28	86.56	42.88	85.76
300	52.88	88.14	52.84	88.07	52.58	87.63

Table 7. The results of the isotherm tests for the adsorption capacity of the Langmuir equation using MDWTR of three distinct particle sizes

Isotherm parameter	Parameter	MDWTR-S	MDWTR-M	MDWTR-L
Langmuir	q_{max} (mg/g)	4.47	4.37	4.32
	K_L (L/mg)	0.127	0.117	0.088
	R_L	0.612	0.631	0.694
	R^2	0.845	0.838	0.856

of chlorophyll-a removal. We observed a robust correlation between PAC dosage and chlorophyll-a removal efficiency. At lower PAC doses (1.5 mg Al/L), there was an increase in chlorophyll-a concentrations, indicating limited effectiveness and even exacerbation of chlorophyll-a presence. However, as the PAC dosage increased to 2.0 mg Al/L and beyond, a remarkable improvement in chlorophyll-a removal efficiency was observed. The highest removal efficiency of 100% was attained at a PAC dosage of 32.0 mg Al/L, indicating complete elimination of chlorophyll-a. These results demonstrate the significant impact of PAC dosage on the removal efficiency of chlorophyll-a from sediment samples (Noyma et al., 2016). The data also revealed consistent pH values across the range of PAC concentrations, indicating a relatively stable pH level (Aksu et al., 2008). However, a clear trend emerged, showing a decrease in pH as the PAC concentration increased (Thongdam et al., 2021) These findings provide robust evidence supporting the effectiveness of PAC in wastewater treatment and highlight the importance of optimizing the PAC dosage for efficient chlorophyll-a removal (Song et al., 2021).

In particular, our study focused on the S-type MDWTR, and the results revealed a gradual decrease in pH and zeta potential as the concentration increased. This consistent trend in measurements indicates the reproducibility of the observed effects (Lucena-Silva et al., 2019; Noyma et al., 2016). Such findings instill confidence in the accuracy of our research outcomes. The significant decrease in chlorophyll-a concentration further strengthens the credibility of our results. When MDWTR was combined with PAC, the removal percentage of *Microcystis aeruginosa* showed significant enhancement, reaching a remarkable maximum of 89.88% at 400 mg/L. Similar trends were observed for the M-type and L-type MDWTR, although with slightly lower removal percentages. These findings highlight the reliable performance of MDWTR, particularly at higher concentrations, for the effective removal of *Microcystis aeruginosa* (Arruda et al., 2021; Lürling et al., 2020)The synergistic combination of MDWTR with PAC significantly enhanced the removal efficiency, providing higher percentage removal values (Kuster, Huser, Padungthon, et al., 2021). Overall, these robust findings support the efficacy of MDWTR and its integration with PAC as a promising approach for water treatment and the successful removal of *Microcystis aeruginosa* from water samples. The present study provides valuable insights into the influence of surface area, pore volume, and heavy metal content on the phosphorus adsorption capacity of MDWTR samples with different particle sizes. The observed increase in surface area, particularly in the MDWTR-S sample, indicates enhanced adsorption capacity compared to the Raw-DWTR, suggesting that modifying the surface area of MDWTR can improve its adsorption efficiency (Kuster, Huser, Thongdamrongtham, et al., 2021). Additionally, the presence of micropores further contributes to the adsorption performance of MDWTR samples. These findings align with previous research that has demonstrated the importance of surface area and pore characteristics in adsorption processes (Leofanti et al., n.d.; F. Li et al., 2019). Furthermore, the variations in heavy metal concentrations across the DWTR samples highlight their potential role in influencing the adsorption capacity of MDWTR. Studies have shown that heavy metals can interact with adsorbents and affect their adsorption efficiency (Cavalcante et al., 2022; Wang et al., 2018)]. In the case of MDWTR, heavy metals such as iron, aluminum, and calcium may interact with phosphorus during the adsorption process, impacting its efficiency (Bacelo et al., 2020; Uddin, 2017; Wu et al., 2020). Understanding the influence of heavy metal content in DWTR is therefore crucial for a comprehensive understanding of its adsorption characteristics.

The isotherm analysis conducted in this study confirms the substantial adsorption capacities of the MDWTR samples. The high R^2 values obtained for all MDWTR types indicate a strong correlation between the experimental data and the Langmuir model, validating its suitability for describing the adsorption behavior of MDWTR. These findings are consistent with previous studies that have successfully applied the Langmuir model to describe the adsorption processes of various adsorbents (Azizian et al., 2018; X. Li et al., 2018). The implications of these findings are significant for the development and optimization of phosphorus removal strategies using MDWTR as an adsorbent. Modifying the surface area and pore volume of MDWTR can be a promising approach to enhance its adsorption capacity, as supported by previous studies that have explored the influence of surface area on adsorption performance (Kasprzyk et al., 2021; Zamparas et al., 2020). Moreover, considering the influence

of heavy metal content in DWTR can provide insights into potential interactions and synergistic effects during the adsorption process, aiding in the design and optimization of efficient water treatment systems. This knowledge contributes to a comprehensive understanding of the adsorption behavior of MDWTR and advances the field of water treatment and adsorption processes.

CONCLUSIONS

Our research findings contribute to the optimization of water treatment processes by addressing critical aspects such as PAC dosage, synergistic effects of MDWTR and PAC, and phosphorus adsorption capacity of MDWTR with different particle sizes. The robust correlation observed between PAC dosage and chlorophyll-a removal efficiency underscores the importance of optimizing PAC dosage for the effective removal of contaminants. The reliable performance of MDWTR, both individually and in combination with PAC, in removing *Microcystis aeruginosa* highlights its potential as a promising approach for water treatment. Additionally, the substantial phosphorus adsorption capacities of MDWTR samples provide valuable options for phosphorus removal in areas where phosphorus pollution is a concern. These findings contribute to the advancement of knowledge in the field of water treatment and offer practical implications for optimizing treatment strategies and expanding the repertoire of effective adsorbents, ultimately leading to improved water quality and environmental sustainability.

Acknowledgments

The research was conducted on behalf of the executive officers and regional authorities with funding from Ubon Ratchathani University and in collaboration with the Office of Physical and Environmental Management, which facilitated water sample collection. The Ubon Ratchathani Provincial Waterworks Authority has provided water samples for scientific research.

REFERENCES

1. Abu-Hasan, H., Muhammad, M.H., Ismail, N.I. 2020. A review of biological drinking water treatment technologies for contaminants removal from polluted water resources. Journal of Water Process Engineering, 33,101035.
2. Adeyemo, A.A., Adeoye, I.O., Bello, O.S. 2017. Adsorption of dyes using different types of clay: a review. Applied Water Science, 7(2), 543–568.
3. Aksu, Z., Tatli, A.I., Tunç, Ö. 2008. A comparative adsorption/biosorption study of Acid Blue 161: Effect of temperature on equilibrium and kinetic parameters. Chemical Engineering Journal, 142(1), 23–39.
4. Alawamleh, H.S.K., Mousavi, S., Ashoori, D., Salman, H.M., Zahmatkesh, S., Sillanpää, M. 2023. Wastewater management using coagulation and surface adsorption through different polyferrics in the presence of TiO_2-g-PMAA particles. Water, 15(1), 145.
5. Arruda, R.S., Pessoa Noyma, N., De Magalhães, L., Coelho, M., Mesquita, B., Costa De Almeida, É., Pinto, E., Lürling, M., Marinho, M.M. 2021. "Floc and Sink" technique removes cyanobacteria and microcystins from tropical reservoir. Water, 13(6), 405.
6. Azizian, S., Eris, S., Wilson, L.D. 2018. Re-evaluation of the century-old Langmuir isotherm for modeling adsorption phenomena in solution. Chemical Physics, 513, 99–104.
7. Bacelo, H., Pintor, A.M.A., Santos, S.C.R., Boaventura, R.A.R., Botelho, C.M.S. 2020. Performance and prospects of different adsorbents for phosphorus uptake and recovery from water. Chemical Engineering Journal, 381, 122566.
8. Backer, L.C., Manassaram-Baptiste, D., LePrell, R., Bolton, B. 2015. Cyanobacteria and algae blooms: Review of health and environmental data from the harmful algal bloom-related illness surveillance system (HABISS) 2007–2011, Toxins, 7(4), 1048–1064.
9. Briand, E., Escoffier, N., Straub, C., Sabart, M., Quiblier, C., Humbert, J.F. 2009. Spatiotemporal changes in the genetic diversity of a bloom-forming Microcystis aeruginosa (cyanobacteria) population. ISME Journal, 3(4), 419–429.
10. Bricker, S.B., Longstaff, B., Dennison, W., Jones, A., Boicourt, K., Wicks, C., Woerner, J. 2008. Effects of nutrient enrichment in the nation's estuaries: A decade of change. Harmful Algae, 8(1), 21–32.
11. Brooks, B.W., Lazorchak, J.M., Howard, M.D.A., Johnson, M.V.V., Morton, S.L., Perkins, D.A.K., Reavie, E.D., Scott, G.I., Smith, S.A., Steevens, J.A. 2016. Are harmful algal blooms becoming the greatest inland water quality threat to public health and aquatic ecosystems? Environmental Toxicology and Chemistry, 35(1), 6–13.
12. Cavalcante, H., Araújo, F., Becker, V., Lucena-Barbosa, J.E. 2022. Control of internal phosphorus loading using coagulants and clays in water and the sediment of a semiarid reservoir susceptible to resuspension. Hydrobiologia, 849, 4059–4071.

13. Kasprzyk, M., Czerwionka, K., Gajewska, M. 2021. Waste materials assessment for phosphorus adsorption toward sustainable application in circular economy. Resources, Conservation and Recycling, 168, 105335.
14. Kuster, A.C., Huser, B.J., Padungthon, S., Junggoth, R., Kuster, A.T. 2021. Washing and heat treatment of aluminum-based drinking water treatment residuals to optimize phosphorus sorption and nitrogen leaching: Considerations for lake restoration. Water, 13(18), 2465.
15. Kuster, A.C., Huser, B.J., Thongdamrongtham, S., Padungthon, S., Junggoth, R., Kuster, A.T. 2021. Drinking water treatment residual as a ballast to sink Microcystis cyanobacteria and inactivate phosphorus in tropical lake water. Water Research, 207, 117792.
16. Leofanti, G., Padovan, M., Tozzola, G., Venturelli, B. 1998. Surface area and pore texture of catalysts. Catalysis Today, 41(1-3), 207-219.
17. Li, F., Wang, M., Liu, S., Hao, Y. 2019. Pore characteristics and influencing factors of different types of shales. Marine and Petroleum Geology, 102, 391–401.
18. Li, X., Cui, J., Pei, Y. 2018. Granulation of drinking water treatment residuals as applicable media for phosphorus removal. Journal of Environmental Management, 213, 36–46.
19. Liu, B., Qu, F., Liang, H., Van der Bruggen, B., Cheng, X., Yu, H., Xu, G., Li, G. 2017. Microcystis aeruginosa-laden surface water treatment using ultrafiltration: Membrane fouling, cell integrity and extracellular organic matter rejection. Water Research, 112, 83–92.
20. Lucena-Silva, D., Molozzi, J., Severiano, J. dos S., Becker, V., Lucena Barbosa, J.E. de. 2019. Removal efficiency of phosphorus, cyanobacteria and cyanotoxins by the "flock & sink" mitigation technique in semi-arid eutrophic waters. Water Research, 159, 262–273.
21. Lürling, M., Kang, L., Mucci, M., van Oosterhout, F., Noyma, N.P., Miranda, M., Huszar, V.L.M., Waajen, G., Marinho, M.M. 2020. Coagulation and precipitation of cyanobacterial blooms. Ecological Engineering, 158, 106032.
22. Matilainen, A., Vepsäläinen, M., Sillanpää, M. 2010. Natural organic matter removal by coagulation during drinking water treatment: A review. Advances Colloid and Interface Science, 159(2), 189–197.
23. Mowe, M.A.D., Mitrovic, S.M., Lim, R.P., Furey, A., Yeo, D.C.J. 2015. Tropical cyanobacterial blooms: A review of prevalence, problem taxa, toxins and influencing environmental factors. Journal of Limnology, 74(2), 205–224.
24. Noyma, N.P., de Magalhães, L., Furtado, L.L., Mucci, M., van Oosterhout, F., Huszar, V.L.M., Marinho, M.M., Lürling, M. 2016. Controlling cyanobacterial blooms through effective flocculation and sedimentation with combined use of flocculants and phosphorus adsorbing natural soil and modified clay. Water Research, 97, 26–38.
25. Pj, O., Botha, A.-M., Ju, G. 2004. Microcystis aeruginosa: source of toxic microcystins in drinking water. African Journal of Biotechnology, 3(3), 159–168.
26. Rice, E.W., Bridgewater, L., 2012. Standard methods for the examination of water and wastewater. American Public Health Association, Washington, DC.
27. Rollwagen-Bollens, G., Connelly, K.A., Bollens, S. M., Zimmerman, J., Coker, A. 2022. Nutrient control of phytoplankton abundance and biomass, and microplankton assemblage structure in the lower Columbia river (Vancouver, Washington, USA). Water, 14(10), 1599.
28. Shen, C., Zhao, Y., Li, W., Yang, Y., Liu, R., Morgen, D. 2019. Global profile of heavy metals and semimetals adsorption using drinking water treatment residual. Chemical Engineering Journal, 372, 1019–1027.
29. Song, W., Xie, Y., Hu, J., Wu, X., Li, X. 2021. Parametric optimization of cyanobacterial coagulation at exponential and decline phases by combining polyaluminum chloride and cationic polyacrylamide. Aqua Water Infrastructure, Ecosystems and Society, 70(3), 317–327.
30. Sukenik, A., Kaplan, A. 2021. Cyanobacterial harmful algal blooms in aquatic ecosystems: A comprehensive outlook on current and emerging mitigation and control approaches. Microorganisms, 9(7), 1472.
31. Sultana, S., Karmaker, B., Saifullah, A.S.M., Galal Uddin, M., Moniruzzaman, M. 2022. Environment-friendly clay coagulant aid for wastewater treatment. Applied Water Science, 12(1), 6.
32. Thongdam, S., Kuster, A.C., Huser, B.J., Kuster, A.T. 2021. Low dose coagulant and local soil ballast effectively remove cyanobacteria (Microcystis) from tropical lake water without cell damage. Water, 13(2), 111.
33. Tian, C., Zhao, Y.X. 2021. Dosage and pH dependence of coagulation with polytitanium salts for the treatment of Microcystis aeruginosa-laden and Microcystis wesenbergii-laden surface water: The influence of basicity. Journal of Water Process Engineering, 39, 101726.
34. Uddin, M. K. 2017. A review on the adsorption of heavy metals by clay minerals, with special focus on the past decade. Chemical Engineering Journal, 308, 438–462.
35. Wang, C., Jiang, H.L., Yuan, N., Pei, Y., Yan, Z. 2016. Tuning the adsorptive properties of drinking water treatment residue via oxygen-limited heat

treatment for environmental recycle. Chemical Engineering Journal, 284, 571–581.

36. Wang, C., Wu, Y., Bai, L., Zhao, Y., Yan, Z., Jiang, H., Liu, X. 2018. Recycling of drinking water treatment residue as an additional medium in columns for effective P removal from eutrophic surface water. Journal of Environmental Management, 217, 363–372.
37. Wu, B., Wan, J., Zhang, Y., Pan, B., Lo, I. M.C. 2020). Selective Phosphate Removal from Water and Wastewater using Sorption: Process Fundamentals and Removal Mechanisms. Environmental Science and Technology. American Chemical Society, 54(1), 50–66.
38. Zamparas, M., Kyriakopoulos, G.L., Drosos, M., Kapsalis, V.C., Kalavrouziotis, I.K. 2020. Novel composite materials for lake restoration: A new approach impacting on ecology and circular economy. Sustainability, 12(8), 3397.
39. Zhong, F., Liu, W., Lv, M., Deng, Z., Wu, J., Cheng, S., Ji, H. 2018. The use of vertical flow constructed wetlands for the treatment of hyper-eutrophic water bodies with dense cyanobacterial blooms. Water Science and Technology, 77(5), 1186–1195.
40. Zhou, X., He, Y., Li, H., Wei, Y., Zhao, L., Yang, G., Chen, X. 2020. Using flocculation and subsequent biomanipulation to control microcystis blooms: A laboratory study. Harmful Algae, 99, 101917.
41. Zhou, Y., Li, X., Xia, Q., Dai, R. 2020. Transcriptomic survey on the microcystins production and growth of Microcystis aeruginosa under nitrogen starvation. Science of the Total Environment, 700, 134501.